FLUID CHARACTERIZATION OF COPPER CONVERTERS

Cesar Real[a], Luis Hoyos[b], Francisco Cervantes[b], Raul Miranda[c], Manuel Palomar-Pardave[a], Miguel Barron[a], Jesus Gonzalez[b]

[a]Departamento de Materiales, [b]Departamento de Sistemas, [c]Departamento de Electrónica
División de Ciencias Básicas e Ingeniería, Universidad Autónoma Metropolitana – Azcapotzalco,
Av. San Pablo 180, Col. Reynosa-Tamaulipas, Del. Azcapotzalco, C. P. 02200, México, D.F., México.
gtji@correo.azc.uam.mx, http://www.azc.uam.mx

Keywords: Peirce-Smith converter, copper reactor, bottom injection, CFD simulations.

Abstract. Peirce-Smith converters (PSC) are used to obtain almost 90% of the blister copper. PSC are long cylindrical chemical reactors where copper matte reacts with air. Traditionally, air is injected laterally through submerged tuyeres at different subsonic velocities. There are several works on which the fluid flow patterns inside the PSC are analyzed by means computational fluid dynamics (CFD) tools. Also, several papers have studied the converter using physical water based models. Numerous authors agree that the most important factors are bath depth and tuyere submergence. Nevertheless, air injection at the converter bottom has not been fully characterized. The aim of bottom injection is to maximize the copper kinetic energy meanwhile avoiding excessive reactor splashing. In this work, a PSC with bottom air injection is studied by means of multiphase 3D CFD numerical simulations considering multiple air velocities. A bubbling regime is displayed at low inlet velocity simulations. As inlet velocity is increased, a transition to a jetting regime is obtained. However, a new transition to the bubbling regime is observed when air is increased again. The unexpected transition is explained in terms of bubble geometry close to the tuyere exit and metalostatic pressure, which directly depends on the copper matte height. An almost linear relationship between copper matte kinetic energy and inlet air velocity is observed. However, the lowest mixing efficiency is obtained at a medium inlet air velocity.

1   INTRODUCTION

Peirce-Smith converters (PSC) are long cylindrical horizontal chemical reactors where air is injected into a copper matte through submerged tuyeres. PSC have been used for decades and today, more than 90% of the world's blister copper is produced in this reactor. To maintain PSC operating correctly, high turbulent conditions inside the reactor are required. Therefore, the process optimization requires that the fluid flow inside the PSC must be fully characterized.

Early works used physical experiments to elucidate the bubbling to jetting flow regimes (Hoefele and Brimacombe, 1979; Brimacombe et al., 1984). The influence of bath depth and tuyere submergence on the formation of standing waves was analyzed by means of water modeling in a subsequent work (Liow and Gray, 1990).

Today, computational fluid dynamics (CFD) is the most common technique use to analyze the Peirce-Smith converter operations, including gas injection, fluid flow during skimming, and gas dynamics within and around the converter hoods (Solnordal, et al., 2006; Vaarno, et al., 1997; Valencia et al., 2004; Valencia et al., 2006; Wing et al., 2005).

Using CFD technique, Vaarno et al. (1997) simulated the isothermal flow field in a PSC. Their numerical results were compared to results that were obtained in a 1/4 scale water model. They found that the presence of relatively large bubbles increase the turbulence in the molten metal.

Traditionally in current PSC, air is injected laterally through submerged tuyeres at different subsonic velocities. However, the accumulated experience in steelmaking, particularly in the basic oxygen furnace (BOF) process, shows that the gas bottom injection may improve the mixing efficiency of a liquid pool.

When gas is injected from a single orifice at the bottom of a liquid pool, two main gas flow regimes can be identified, bubbling and jetting. At low gas velocities, discrete bubbles are formed from the orifice, marking the single bubbling regime. At high gas velocities, a coherent gas jet forms with small bubbles split at the end of the jet, marking the jetting regime. Between the single bubbling and jetting regimes, a transition regime exists, which is known as doubling or coalesced bubbling regime (Kulkarni and Joshi, 2005).

The aim of this work is to explore the bottom injection as an alternative technique, to improve the mixing efficiency in PSC. Isothermal 3-D numerical simulations of a segment, of an industrial PSC employing bottom injection were carried out. The commercial CFD software Fluent was employed to solve the transient Navier-Stokes equations. The K-ε turbulence model and the volume of fluid model (VOF) were used in order to model the turbulent nature of the flow and to deal with the multiphase flow. Four different air velocities were studied. Special attention was paid to the bubbles formation mechanism. The mixing efficiency was measured by calculating the turbulent kinetic energy of the copper matte.

2   MATHEMATICAL MODEL

2.1 The VOF model

The VOF model is a surface-tracking technique applied to a fixed Eulerian mesh. In other words, the VOF is an Euler-Euler model. The different phases are treated mathematically as interpenetrating continua in this model. Since the volume of a phase cannot be occupied by the other phases, the concept of phasic volume fraction is introduced. In each control volume, the volume fractions of all phases sum to unity. The field for all variables and properties are shared by the phases and represent volume-averaged values, as long as the volume fraction of

each of the phases is known at each location. Thus the variables and properties in any given cell are either purely representative of one of the phase, or representative of a mixture of phases, depending upon the volume fraction values. In other words, if the qth fluid's volume fraction in the cell is denoted as α_q, then the following three conditions are possible:

$\alpha_q = 0$:   The cell is empty (of the qth fluid)
$\alpha_q = 1$:   The cell is full (of the qth fluid)
$0 < \alpha_q < 1$:   The cell contains the interface between the qth fluid and one or more other fluids.

Based on the local value of α_q, the appropriate properties and variables will be assigned to each control volume within the domain.

2.2 Volume fraction equation

In the VOF model, the tracking of the interfaces between the phases is accomplished by the solution of a continuity equation for the volume fraction of one (or more) of the phases. For the qth phase, this equation has the following form:

$$\frac{\partial}{\partial t}\left(\alpha_q \rho_q\right) + \nabla \cdot \left(\alpha_q \rho_q \vec{v}_q\right) = 0 \tag{1}$$

In the VOF model, the volume fraction equation for the primary phase is not solved. The volume fraction of the primary phase (air in this work) is computed based on the following constraint:

$$\sum_{q=1}^{n} \alpha_q = 1 \tag{2}$$

2.3 Momentum equation

A single momentum equation is solved throughout the domain, and the resulting velocity field is shared among the phases.

$$\frac{\partial}{\partial t}\left(\rho \vec{v}\right) + \nabla \cdot \left(\rho \vec{v} \vec{v}\right) = -\nabla p + \nabla \cdot \left[\mu\left(\nabla \vec{v}\right) + \nabla \vec{v}^T\right] + \rho \vec{g} + \vec{F} \tag{3}$$

The control-volume formulation requires that convection and diffusion fluxes through the control volume faces be computed and balanced with source terms within the control volume itself. The scheme calculation of face fluxes in the VOF model is the Euler explicit approach.

The properties appearing in the transport equation (3) are determined by the presence of the component phase in each control volume. In a two phase system, for example, if the phases are represented by the subscripts 1 and 2 and the volume fraction of the second of these is being tracked, the density in each cell is given by:

$$\rho = \alpha_2 \rho_2 + \left(1 - \alpha_2\right)\rho_1 \tag{4}$$

All other properties (e.g., viscosity) are computed in this manner.
To consider the turbulent effects in simulating the fluid flow inside the PSC, the standard

K−ε model was employed. In the VOF model, the turbulence variables K and ε are shared by the phases throughout the field.

3 SYSTEM DESCRIPTION

Figure 1 depicts a sketch of the copper converter with bottom injection employed in the computer simulations. Dimensions of a typical current PSC are presented in Table 1 (Vaarno et al., 1997). This table also shows the dimensions of the model and the fluids physical properties used in this work. An initial bath depth of 1.0 m was considered.
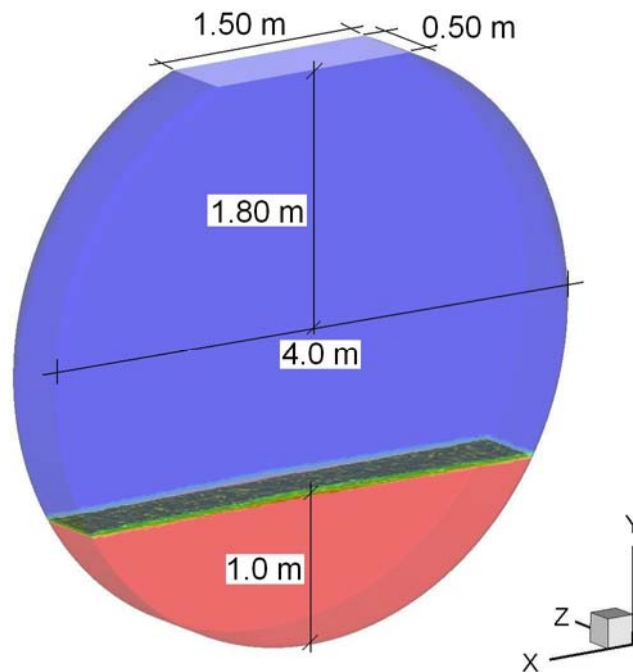

Figure 1: Schematic representation of the PSC slice.

The system must be discretized using a very fine mesh, to reproduce accurately bubble formation. However due to the mesh size, the simulation of the entire converter is not feasible. Therefore, only a slice of the converter was simulated (see Figure 1). The system modeled had 1,824,677 elements. The PSC and model tuyere areas were not identical due to the mesh size, but the effective areas are close enough to ensure the PSC and model air inlet flows are the same.

For simplicity, all converter walls were modeled as rigid no slip ones. This model for the wide walls is unrealistic. However, more realistic boundary conditions like symmetry or periodic will be presented in a future work.

In the 3D transient numerical simulations two phases were taken into account, namely copper mate and air. A time step of 0.001 s was used given that this value was sufficient to keep the numerical convergence and stability. Four air velocities were considered in this work and their values are reported in Table 2. Considering that in current typical PSC the inlet air velocity is 150 m/s, the velocities used in Cases A, B, C, and D correspond to 3.33%, 50%, 66.67%, and 100%, respectively, of this current value.

	PSC	Model
Copper viscosity (Pa s)	0.01	0.01
Copper density (kg/m^3)	4600	4600
Copper temperature (K)	1493	1493
Copper bath height (m)	1.0	1.0
Gas density (kg/m^3)	1.2	1.2
Inlet gas velocity (m/s)	150	5, 75, 100, 150
Converter inner diameter (m)	3.5	4.0
Converter length (m)	9.14	0.5
Tuyeres number	42	1
Tuyeres submergence (m)	0.52	1.00
Tuyeres diameter (m)	0.041	0.045
Tuyeres spacing (m)	0.205	

Table 1: Fluids physical properties and dimensions of a current PSC and the model.

The air velocity in Case A is extremely low, but it allows for the understanding of bubble formation mechanism. Clearly, this velocity can not replace the lateral air injection in the PSC.

Case	Air velocity (m/s)
A	5.0
B	75.0
C	100.0
D	150.0

Table 2: Air velocities studied in this work.

4 RESULTS

4.1 Flow patterns inside the PSC

The fluid flow pattern inside the PSC slice, with inflow air velocities of 5, 75, 100 and 150 m/s respectively is shown in Figures 2-5. To highlight the main features of the fluid flow pattern inside the PSC, the numerical results are reported at different simulation times in each case.

A bubbling regime was obtained when the PSC inlet air velocity was 5 m/s, as shown in Figure 2. The sizes of the bubbles observed were small. From Figures 2d-2f it is clear that the bubbles formation is a periodical process. The similarity of Figure 2e and Figure 2f confirms this. However, the determination of the bubbles formation frequency was not taken into account.

Due to the metallostatic pressure the shapes of the bubbles were not spherical, but rather elongated. As the bubbles rise, their shapes became more spherical. At higher PSC inlet air velocities, this fact will become very important.
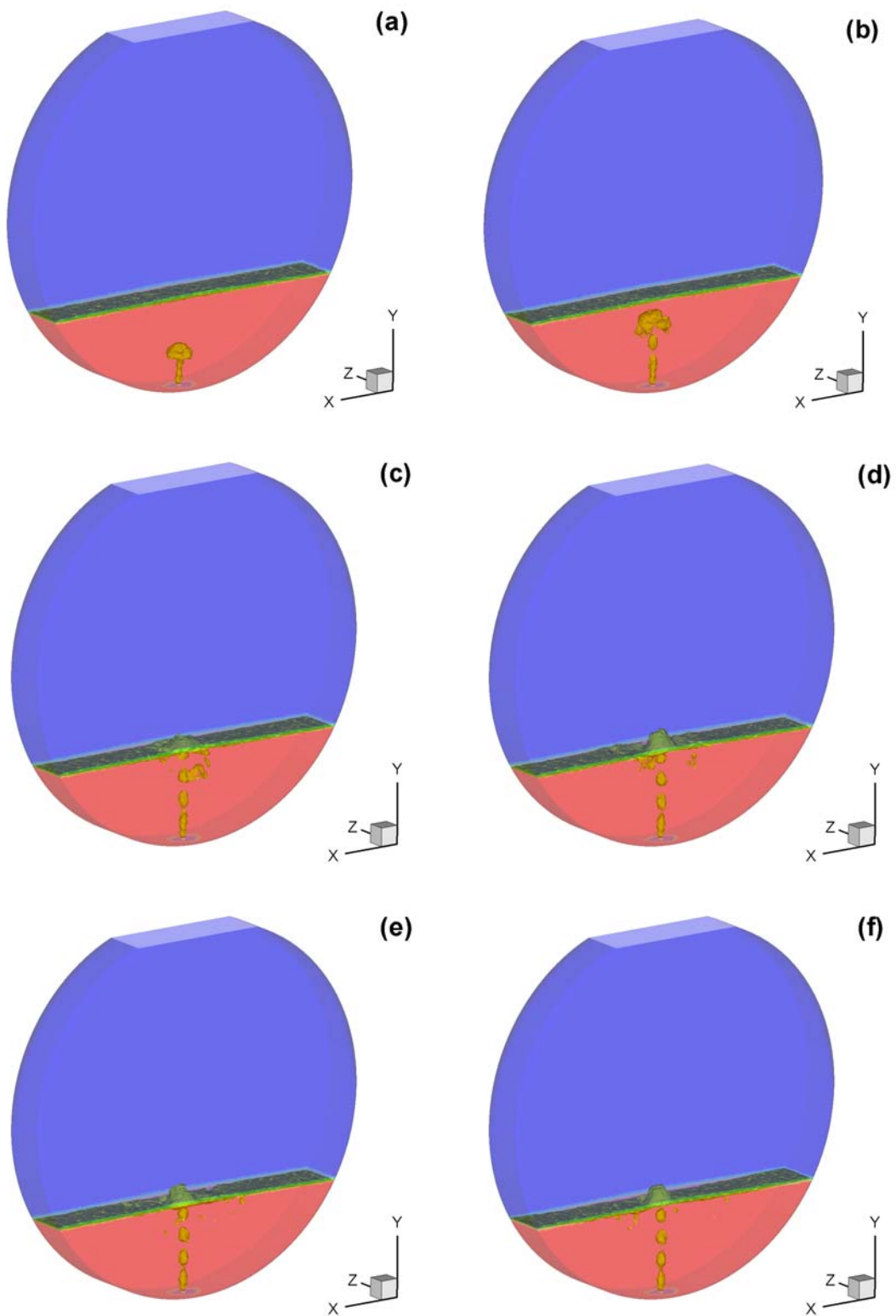
Figure 2: Fluid flow behavior inside the PSC in Case A. (a) 0.6s, (b) 1.1s, (c) 1.6s, (d) 2.1s, (e) 2.6s, (f) 3.1s.

The copper matte free surface remains almost unaltered in Case A. This signifies that only a small amount of the air kinetic energy is transmitted to the copper mate. In the next subsection the liquid kinetic energy will be evaluated.
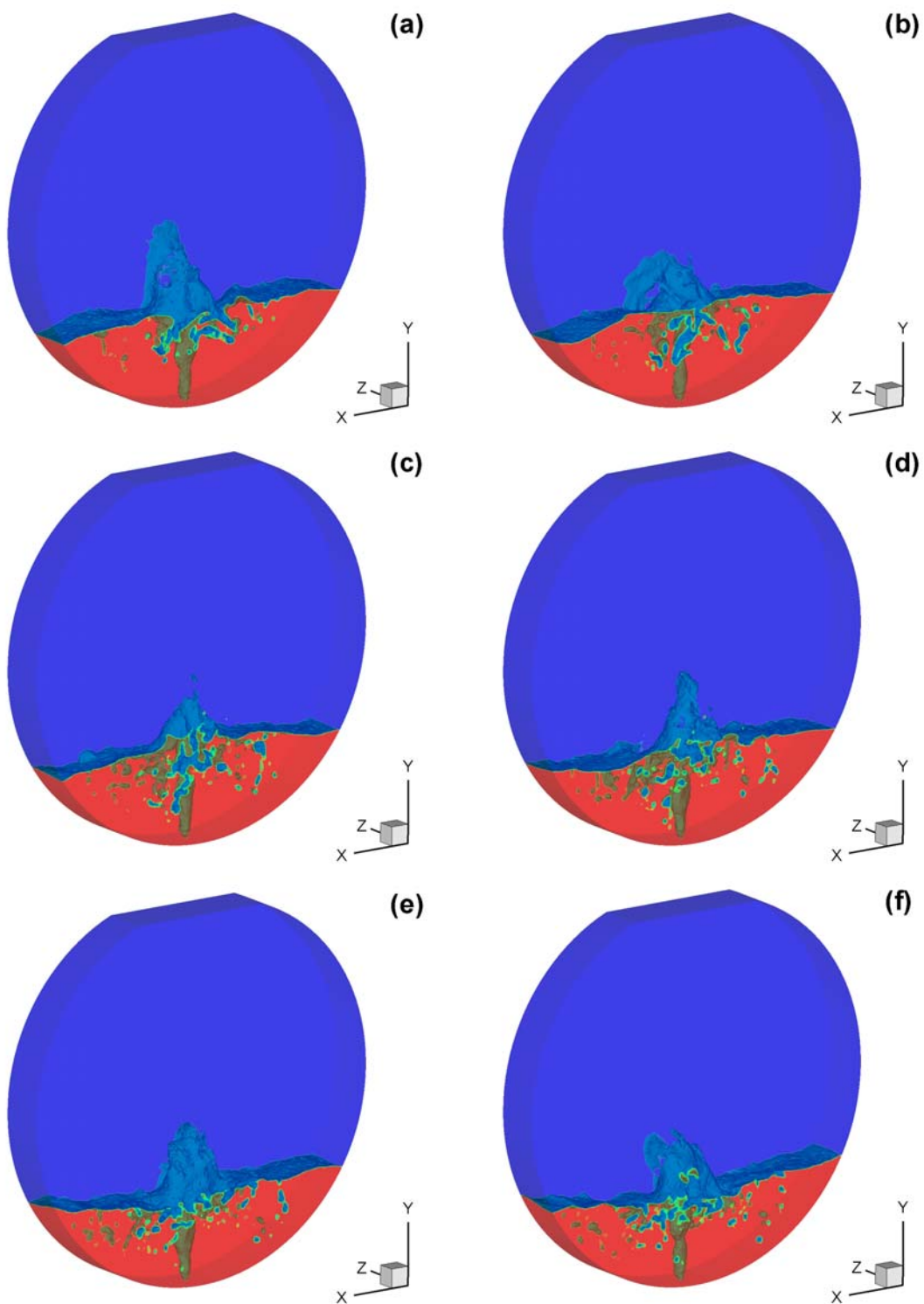
Figure 3: Fluid flow behavior inside the PSC in Case B. (a) 3.0s, (b) 3.2s, (c) 3.4s, (d) 3.6s, (e) 3.8s, (f) 4.0s.

The dynamic behavior inside the PSC for Case B, once the process has reached stable conditions is shown in Figure 3. With this air inlet velocity a jetting regime was obtained. This jetting regime becomes evident in the next subsection. The transition from bubbling to

jetting regime is not surprising, given that Case B air velocity was fifteen times Case A. In the jetting regime it is almost impossible to observe a periodical behavior of the flow pattern inside the PSC.
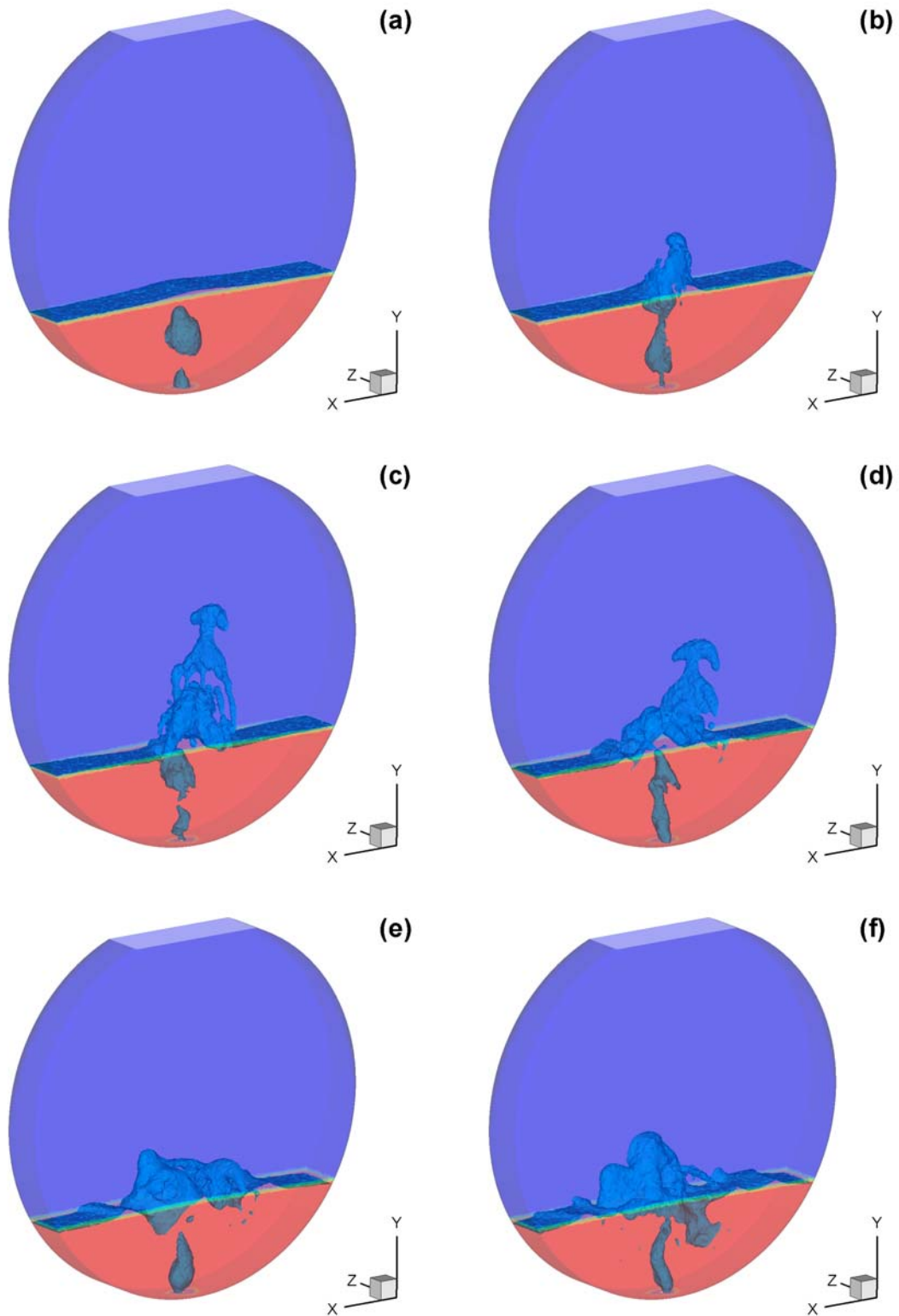
Figure 4: Fluid flow behavior inside the PSC in Case C. (a) 0.3s, (b) 0.5s, (c) 0.9s, (d) 1.2s, (e) 1.4s, (f) 1.6s.
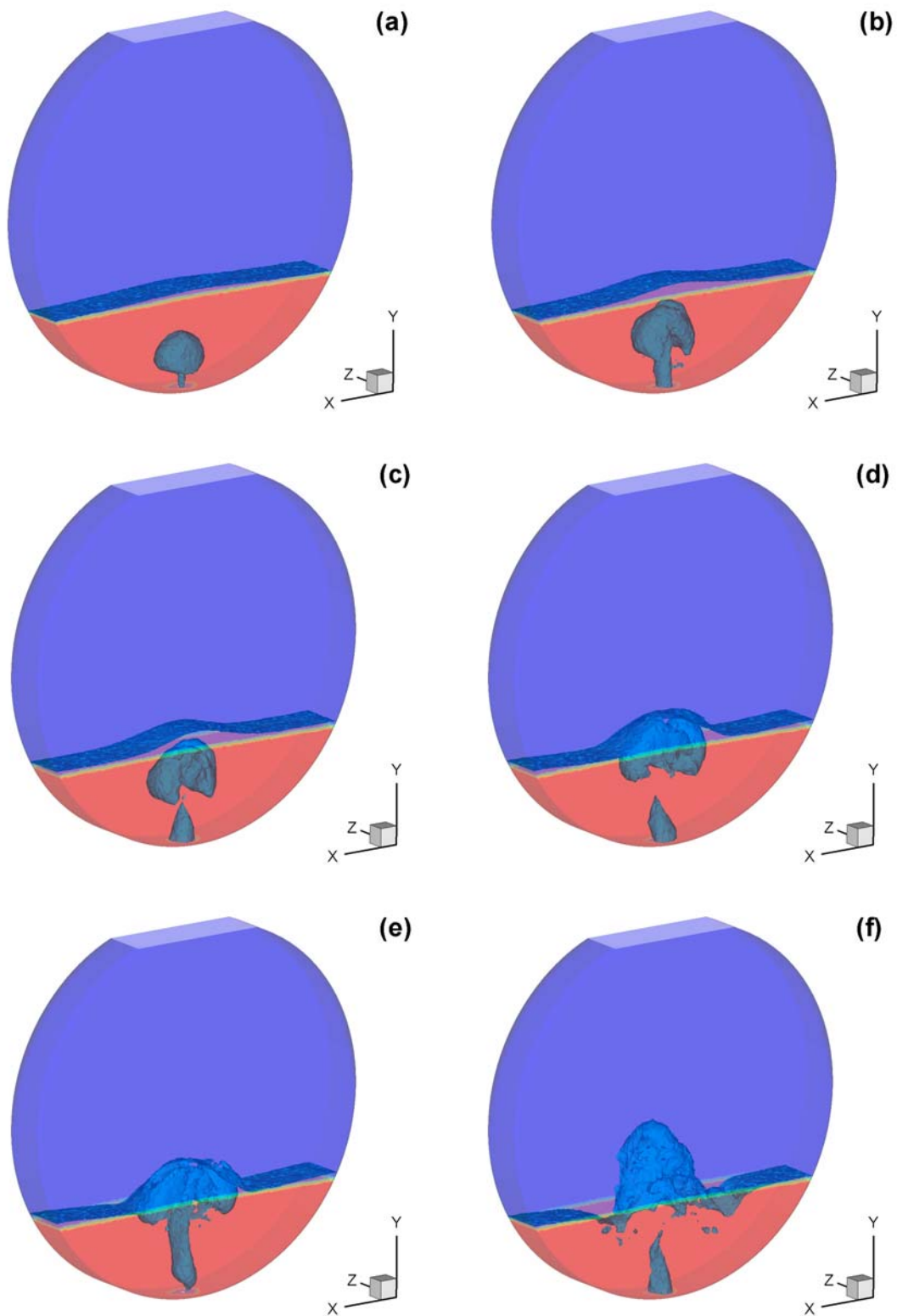
Figure 5: Fluid flow behavior inside the PSC in Case D. (a) 0.3s, (b) 0.5s, (c) 0.6s, (d) 0.8s, (e) 0.9s, (f) 1.2s.

The copper matte free surface deformation shown in Figures 3e-3f suggests strong mixing inside the PSC, but the copper splashing was not severe. The height of the upper copper drops does not surpass the middle of the PSC.

It is important to notice that plume base is close to the tuyere area, but the plume transversal section increases rapidly. Air jet collides against the PSC wide walls just below the copper mate free surface. The PSC slice wide walls were modeled as rigid ones. Perhaps different results could be obtained if they were modeled as symmetry boundaries. Moreover, given that the current PSC had several tuyeres, the interaction between neighbouring air jets could be considerable. This situation will be studied in a future work.
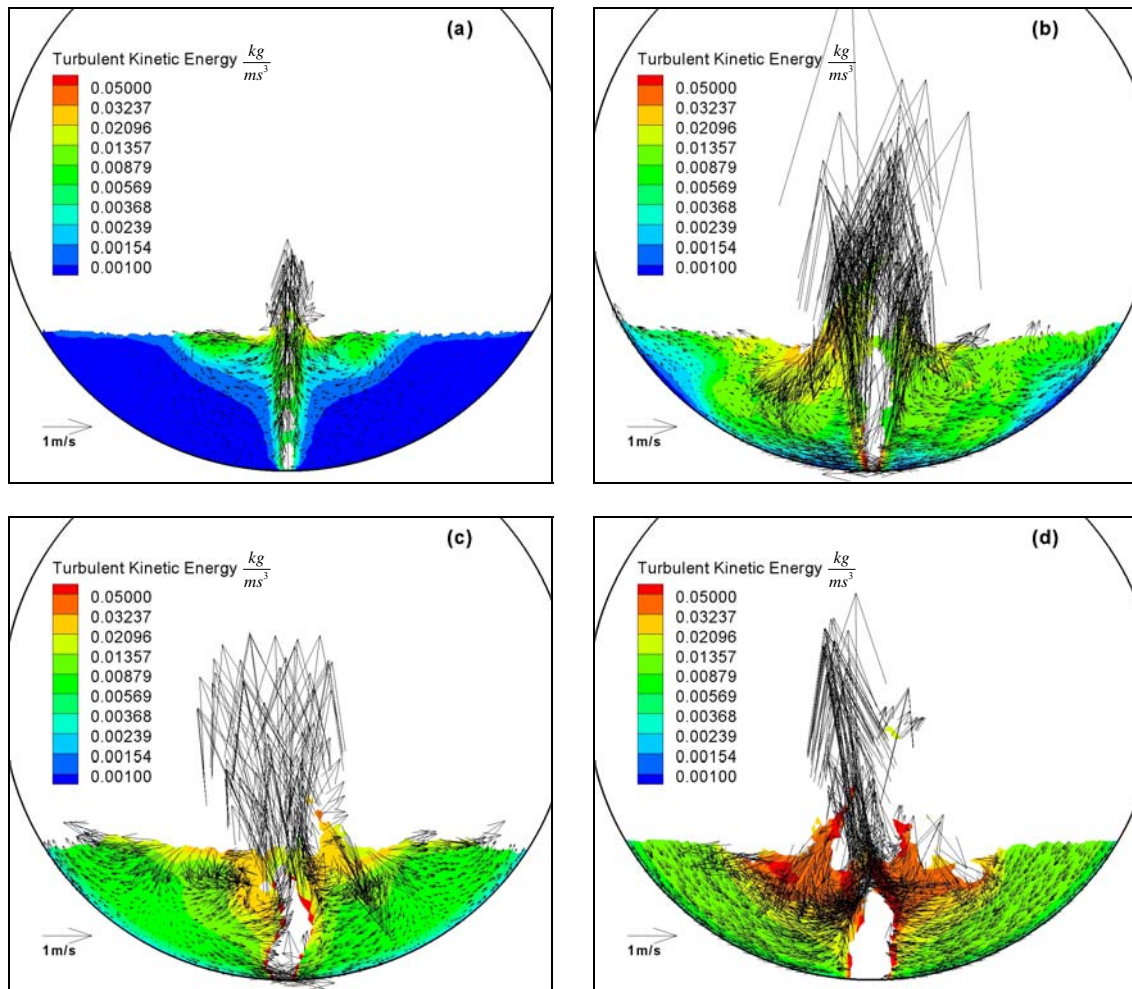

Figure 6: Contours of turbulent kinetic energy and velocity vector field in the XY central plane for each case.
(a) Case A. (b) Case B. (c) Case C. (d) Case D.

The dynamic behavior inside the PSC for Case C and Case D are shown in Figures 4 and 5 respectively. The early stages of the air injection are shown in these figures. A rare result was obtained. A new transition from jetting to bubbling regime was observed in both cases.

In reality, the regime observed in Case C is a combination of bubbling and jetting regimes. The presence of the bubbling-jetting regimes may be explained by taking into account the liquid copper metallostatic pressure and bubbles formation mechanism.

Given that in Cases C and D the inlet velocity was very high, the air jet emerging from the tuyere was very slender, and did not support the copper matte metallostatic pressure. This explains the difference in bubble lengths measured vertically. In Case C bubbles are larger than in Case D. This phenomenon produces different bubbles shapes in each case. In case C, bubbles emerging from the tuyere resembled elongated spheres. On the other hand, bubbles at

the PSC bottom for Case D resembled wide base cones.

This difference in the lengths allows the contact between floating and emerging bubbles as shown in Case C. When the joined bubbles reach the copper matte surface, an open jet regime appears. This explains the reason the copper splashing in Case C is bigger than in Case D. When copper matte metallostatic pressure cuts the gas jet the jetting regime stopped.

The previous analysis is strengthened by a previous work done by Ozawa and Mori (1986), which reported that system pressure or gas density had a significant effect on the bubbling–jetting transition. Ozawa and Mori also studied the effects of the physical properties of gas and liquid on the bubbling–jetting transition in liquids. They found that the bubbling–jetting transition occurs at lower gas velocities when the ratio of gas to liquid densities was increased.

4.2 Mixing evaluation

The aim of the bottom air injection proposed in this work was to maximize the copper kinetic energy, while avoiding excessive reactor splashing. In the previous section the fluid flow behavior inside the PSC and the copper splashing were analyzed. The analysis of the mixing efficiency is done in this section.
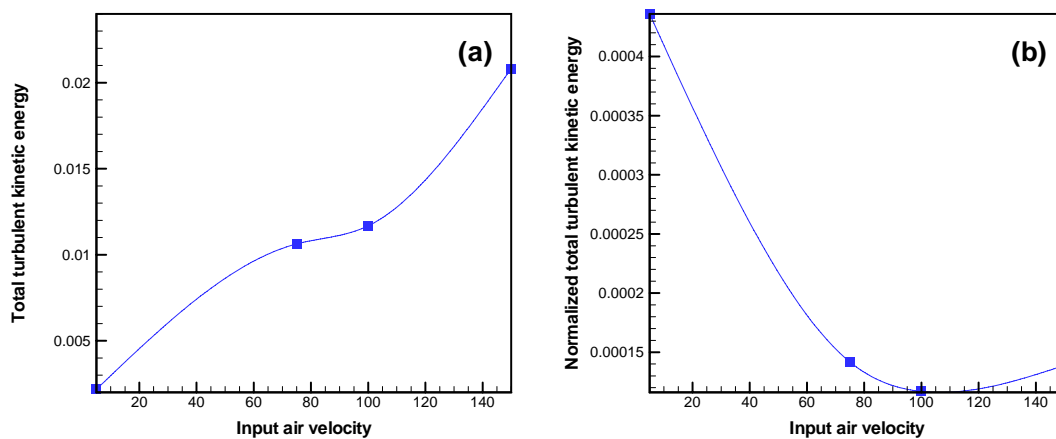

Figure 7: Total and normalized turbulent kinetic energy for each Case.

Different criteria have been used to identify the bubbling–jetting transition and to evaluate the liquid mixing efficiency in processes like the PSC. The turbulent kinetic energy was used in this work to quantify the copper matte mixing. Figure 6 shows the contours of turbulent kinetic energy on the central XY plane for Cases A, B, C and D. The regions containing air were eliminated. The copper matte velocity vectors were included.

The smallest velocity vectors are observed in Figure 6a, and the biggest one are observed in Figure 6b. The difference is due to the flow regime in each Case. Case A had a bubbling regime, while Case B had a jetting regime. In Case B, near the plume, the copper velocity is high, while at a further distance from the plume the copper velocity is low.

The integral of the turbulent kinetic energy over the copper matte volume versus the inlet air velocity is shown in Figure 7a. The relationship between the total kinetic energy and the inlet air velocity is almost linear. This result is not unexpected, the higher the inlet air velocity, the higher the copper mate velocity.

To normalize the copper mixing inside the PSC, the integral of the turbulent kinetic energy

was divided by the inlet air velocity. The results of these calculations are shown in Figure 7b. It can be observed that the normalized turbulent kinetic energy displayed a minimum value at Case C. In other words, the lowest copper matte mixing efficiency was obtained in Case C.

5   CONCLUSIONS

In this work, the fluid flow behavior inside a PSC using bottom air injection was studied. Different air velocities were considered. At low inlet air velocities, a bubbling regime was obtained. As the air velocity increases, a bubbling-jetting transition occurs.

The lowest copper matte mixing efficiency was obtained at a medium inlet air velocity. This signifies that very high air velocities are not necessary to obtain adequate copper matte mixing conditions. This result is important given that it is necessary to reduce the PSC fume emissions.

REFERENCES

Brimacombe J.K., Meredith S.E. and Lee R.G.H., High-Pressure Injection of Air into a Peirce-Smith Copper Converter, *Metallurgical and Materials Transactions B*, 15B, 243-250, 1984.

Fluent User's Guide 6.1 Version. *Fluent Incorporated*, Lebanon, NH, 2003.

Hoefele E.O. and Brimacombe J.K., Flow Regimes in Submerged gas Injection, *Metallurgical and Materials Transactions B*, 10B, 631-648, 1979.

Kulkarni A.A. and Joshi J.B., Bubble formation and bubble rise velocity in gas–liquid systems: a review, *Industrial and Engineering Chemistry Research*, 44, 5873–5931, 2005.

Liow J.L. and Gray N.B., Slopping Resulting from Gas Injection in a Peirce-Smith Converter: Water Modelling, *Metallurgical and Materials Transactions B*, 21B, 987-996, 1990.

Ozawa Y. and Mori K., Effect of physical properties of gas and liquid on bubbling–jetting phenomena in gas injection into liquid, *Transactions ISIJ*, 26, 291–297, 1986.

Solnordal C.B., Witt P.J., Manzoori A., Namavari H., Niknejad E. and Davari M., A Correlation-based model for predicting gas extraction performance in a copper converting plant, *JOM,* 51-70, 2006.

Vaarno J., Pitkala J., Ahokainen T. and Jokilaakso A., Modelling Gas Injection of a Peirce-Smith Converter, *Int. Conf. on CFD in Mineral & Metal Processing and Power Generation, CSIRO, Australia*, 297-306, 1997.

Valencia A., Paredes R., Rosales M., Godoy E. and Ortega J., Fluid Dynamics of Submerged Gas Injection into Liquid in a Model of Copper Converter, *Int. Comm. On Heat Mass Transfer,* 31, 21-30, 2004.

Valencia A., Rosales M., Paredes R., Leon C. and Moyano A., Numerical and Experimental Investigation of the Fluid Dynamics in a Teniente Type Copper Converter. *Int. Comm. on Heat Mass Transfer*, 33, 302-310, 2006.

Wing K., Kapusta J.P., Harris R., Wraith A.E. and Parra R., Modelling Peirce-Smith

Converter Operating Cost. *JOM*, 52-57, 2005.